

Specific Adhesion of Membranes: Mapping to an Effective Bond Lattice Gas

Thomas Speck,^{1,2} Ellen Reister,³ and Udo Seifert³

¹*Department of Chemistry, University of California, Berkeley, California 94720, USA*

²*Chemical Sciences Division, Lawrence Berkeley National Laboratory, Berkeley, California 94720, USA*

³*II. Institut für Theoretische Physik, Universität Stuttgart, D-70550 Stuttgart, Germany.*

We theoretically consider specific adhesion of a fluctuating membrane to a hard substrate via the formation of bonds between receptors attached to the substrate and ligands in the membrane. By integrating out the degrees of freedom of the membrane shape, we show that in the biologically relevant limit specific adhesion is well described by a lattice gas model, where lattice sites correspond to bond sites. We derive an explicit expression for the effective bond interactions induced by the thermal undulations of the membrane. Furthermore, we compare kinetic Monte Carlo simulations for our lattice gas model with full dynamic simulations that take into account both the shape fluctuations of the membrane and reactions between receptors and ligands at bond sites. We demonstrate that an appropriate mapping of the height dependent binding and unbinding rates in the full scheme to rates in the lattice gas model leads to good agreement.

PACS numbers:

I. INTRODUCTION

Adhesion of biomembranes to each other is ubiquitous in living organisms since it is *inter alia* crucial for processes like cell signaling or wound healing [1]. While in many cases two membranes may effectively be attracted to each other due to non-specific interactions, like electrostatic or van der Waals interactions, adhesion in biological systems is typically supported by receptors and ligands in the membrane that form bonds upon contact [2–5]. The largest protein families involved in adhesion are cadherins, integrins, and selectins [6]. In order to gain understanding of the processes of specific adhesion much experimental effort has been made to develop model systems using artificially prepared lipid bilayer vesicles with inserted ligands that are brought into the vicinity of receptors tethered to stiff or soft, polymer-cushioned, substrates [7–11].

From a theoretical perspective, membranes are well described as two-dimensional sheets with a bending rigidity and a rather small effective surface tension. This model, first introduced by Helfrich [12], has been successful in describing morphology and dynamics of free lipid bilayers and vesicles [13]. Since membranes are often not free but move close –or adhere– to other membranes (or, in model systems, to substrates) much work has been dedicated to the understanding of non-specific interactions between membranes [14]. In particular, analogies to wetting theory and the character of the transition between bound and unbound membrane [15–18] have been explored. In many studies on adhesion receptor-ligand bonds were integrated out exactly in order to derive an effective interaction potential that depends on the distance between the membranes or between membrane and substrate [19–22]. Other studies employed mean-field approaches that use coarse-grained bond density fields [23, 24]. In all of these approaches the discrete nature of specific adhesion involving receptor-ligand pairs is hidden. It only remains visible in more recent work relying on the use of simu-

lations that typically combine the continuous nature of the membrane with the discrete nature of the adhesion bonds [25–27].

In this work, we follow the opposite strategy compared to previous theoretical studies by integrating out the membrane shape in order to describe adhesion purely through receptor-ligand bonds. Starting from a mixed continuous-discrete model we show that in the regime of confined and rather stiff membranes, which is relevant for cells, it maps onto a lattice gas, where lattice sites correspond to receptor-ligand pairs. Membrane properties enter the effective interactions between bonds. The benefits from such an approach are two-fold: firstly, we can apply the vast knowledge and methods developed for lattice gases to the adhesion behavior of membranes, and, secondly, it allows for the efficient numerical simulation by only taking into account the discrete bonds. We demonstrate in which regime such a pure lattice gas description is valid and explicitly calculate the effective bond interactions. By constructing realistic reaction rates taking into account the distance between the membrane and the substrate, we are capable of qualitatively capturing the

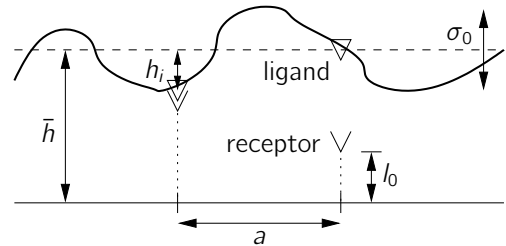


FIG. 1: Sketch of the membrane. Besides non-specific interactions between substrate and membrane, bonds (with rest length l_0) between receptors and ligands embedded into the membrane can form. The mean height of the membrane with respect to the substrate is \bar{h} . Thermal fluctuations of the membrane are of size σ_0 . Above bond i , the deviation of the membrane height profile from the mean height is $\sigma_0 h_i$.

dynamics of adhesion within the lattice gas framework. We support this claim by comparing simulation results for the full Hamiltonian with lattice gas simulations employing the kinetic Monte Carlo method.

II. MODEL AND MAPPING

We consider a fluctuating bio-membrane in a fluid at temperature T above a substrate. The membrane is described in the Monge representation by the height profile $h(\mathbf{r})$ with $\mathbf{r} = (x, y)$. The projected area is A and we employ periodic boundary conditions. In addition, N receptors at positions $\{\mathbf{r}_i\}$ are embedded in the substrate that can bind to the corresponding ligands in the membrane, see Fig. 1.

Our starting point is the total Hamiltonian $\mathcal{H} = \mathcal{H}_0 + \mathcal{H}_{\text{ns}} + \mathcal{H}_{\text{s}}$ composed of three terms [20, 27]. The first term is the Helfrich energy

$$\mathcal{H}_0[h(\mathbf{r})] = \int_A d\mathbf{r} \frac{\kappa}{2} [\nabla^2 h(\mathbf{r})]^2 \quad (1)$$

with bending rigidity κ governing the thermal fluctuations of the membrane. Non-specific interactions between the substrate and the membrane are due to, e.g., surface charges, van der Waals forces, or steric repulsion. They occur over ranges where individual molecules are not resolved. These non-specific interactions are modeled through the simple quadratic potential

$$\mathcal{H}_{\text{ns}}[h(\mathbf{r})] = \int_A d\mathbf{r} \frac{\gamma}{2} [h(\mathbf{r}) - h_0]^2 \quad (2)$$

with strength γ resulting from a Taylor expansion around the minimum at height h_0 . The magnitude of the membrane height fluctuations in the absence of bonds is

$$\begin{aligned} \sigma_0^2 &\equiv \langle [h(0) - \bar{h}]^2 \rangle \\ &= \frac{1}{2\pi\beta} \int_0^\infty dq \frac{q}{\kappa q^4 + \gamma} = \frac{1}{8\beta\sqrt{\gamma\kappa}} \end{aligned} \quad (3)$$

using $\langle |\tilde{h}_{\mathbf{q}}|^2 \rangle = [\beta A(\kappa q^4 + \gamma)]^{-1}$ with $\beta \equiv 1/k_B T$ (see Eq. (A1) for the definition of the Fourier coefficients). Here, \bar{h} is the mean height of the membrane.

The focus of this work lies on specific substrate-membrane interactions through ligand-receptor pairs contributing with

$$\mathcal{H}_{\text{s}}[h(\mathbf{r}); \{b_i\}] = \sum_{i=1}^N b_i \left\{ \frac{k}{2} (\bar{h} + \sigma_0 h_i - l_0)^2 - \epsilon_b \right\} \quad (4)$$

to the total Hamiltonian. This energy is determined by two competing terms, the specific binding energy ϵ_b and the energy stored in a stretched bond with effective spring constant k . The N binary variables b_i are 1 for a closed bond and 0 for an open bond. The bonds have rest length l_0 , and $h(\mathbf{r}_i) \equiv \bar{h} + \sigma_0 h_i$ is the distance of the membrane

ligand at \mathbf{r}_i from the substrate. The dimensionless h_i are of order unity. It will be advantageous to define two more quantities: the (average) area per bond

$$a^2 \equiv A/N$$

and the fraction

$$\phi \equiv \frac{1}{N} \sum_{i=1}^N b_i$$

of closed bonds.

The partition sum reads

$$Z \equiv \sum_{\{b_i\}} \int [dh(\mathbf{r})] e^{-\beta \mathcal{H}[h(\mathbf{r}); \{b_i\}]} \quad (5)$$

Our goal is to derive an effective lattice gas model by integrating out the height field $h(\mathbf{r})$. The integration over the membrane fluctuations under the constraint of given heights h_i is carried out in appendix A,

$$Z \simeq \sum_{\{b_i\}} \int dh_1 \cdots dh_N e^{-\frac{1}{2} \sum_{ij} (m^{-1})_{ij} h_i h_j - \beta E_b}, \quad (6)$$

leading to a coupling of the height variables h_i with coupling matrix

$$m_{ij} \equiv \frac{2}{\beta A \sigma_0^2} \sum_{\mathbf{q} \neq 0} \frac{\cos \mathbf{q} \cdot (\mathbf{r}_i - \mathbf{r}_j)}{\kappa q^4 + \gamma}, \quad (7)$$

where the sum runs over independent wave vectors only. We rewrite the explicit expression for E_b from Eq. (A2) in terms of three dimensionless parameters χ , θ , and λ :

$$\begin{aligned} \beta E_b &= -\frac{1}{2} \frac{[\chi \sum_i b_i h_i - N\theta\lambda]^2}{N\theta + N\phi\chi} \\ &\quad + \frac{1}{2} \theta \lambda^2 + \sum_{i=1}^N b_i \left(\frac{1}{2} \chi h_i^2 - \beta \epsilon_b \right). \end{aligned} \quad (8)$$

Here,

$$\chi \equiv \beta k \sigma_0^2 \quad (9)$$

is an effective cooperativity parameter between bonds discussed further below, while

$$\theta \equiv \beta \gamma a^2 \sigma_0^2 \quad (10)$$

is the average energy contribution from the non-specific potential per bond. Finally, $\lambda \equiv (h_0 - l_0)/\sigma_0$ is the ratio of the distance between the minimum of the non-specific potential and the rest length of the tether, and the amplitude of height fluctuations.

For now we assume that χ is small. Below and in the next section we will demonstrate that this assumption indeed corresponds to the range of parameters we are

interested in. Hence, Taylor-expanding Eq. (8) up to first order in χ we obtain

$$\beta E_b \approx \chi \lambda \sum_{i=1}^N b_i h_i + \sum_{i=1}^N b_i \left[\frac{1}{2} \chi h_i^2 - \beta(\epsilon_b - \epsilon_t) \right]$$

with the typical tether energy

$$\epsilon_t \equiv \frac{k}{2} (h_0 - l_0)^2 = \frac{1}{2} \chi \lambda^2 k_B T. \quad (11)$$

Within this approximation E_b becomes independent of θ . Instead of λ we will take ϵ_t as the independent variable in the following, leaving us with ϵ_t , ϵ_b , and χ . We now perform the Gaussian integration in Eq. (6). To this end, we have to invert the matrix $(m^{-1})_{ij} + \chi b_i \delta_{ij}$, leading to $m_{ij} + \mathcal{O}(\chi)$. Hence, to first order in χ we finally arrive at

$$Z \simeq \sum_{\{b_i\}} \exp \left\{ \beta \sum_{i \neq j} \nu_{ij} b_i b_j + \beta \mu \sum_{i=1}^N b_i \right\} \quad (12)$$

which is isomorphic to the lattice gas model of the liquid-gas transition with a binary density b_i [28]. The sum runs over all bonds where the diagonal term is included in the lattice gas chemical potential

$$\mu \equiv \epsilon_b - \epsilon_t(1 - \chi). \quad (13)$$

The effective interaction energy between bonds is given through

$$\nu_{ij} \equiv \epsilon_t \chi m(|\mathbf{r}_i - \mathbf{r}_j|), \quad m(r) = -\frac{4}{\pi} \text{kei}_0(r/\xi) \quad (14)$$

with length scale

$$\xi \equiv (\kappa/\gamma)^{1/4} = \sqrt{8\beta\kappa} \sigma_0 = \sqrt{8\chi\kappa/k}. \quad (15)$$

For the derivation and form of this effective interaction, see appendix B and Fig. 2.

This mapping from the original full model to an effective bond lattice gas is the central result of this paper valid for any geometry of bonds. The small quantity χ defined in Eq. (9) determines the *local cooperative* interactions of bonds. The physical picture is that a closed bond pulls down the membrane, assisting neighboring bonds to form. We have assumed the local effect of this behavior to be small; either through weak links (small k) such that the deforming force on the membrane is small, or by a stiff, confined membrane (small σ_0) which is rather pulled down as a whole instead of being locally deformed. The membrane mediated interactions between bonds then decay on the length scale ξ , and an effective description in terms of the bonds alone becomes feasible.

III. SQUARE LATTICE: NEAREST-NEIGHBOR APPROXIMATION

For a perfectly flat membrane with $\sigma_0 = 0$ (implying $\chi = 0$) there is no coupling between bonds, i.e., the bonds

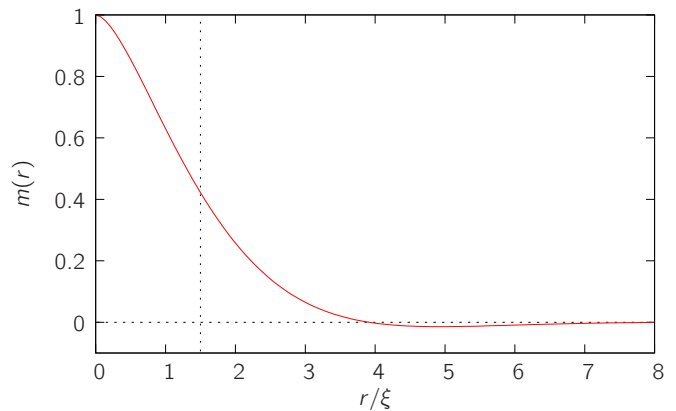


FIG. 2: Decay of the effective membrane-induced interactions $m(r)$ between bonds from Eq. (14). The dotted vertical line marks the bond distance a used for the nearest-neighbor approximation.

are independent. The partition sum is then calculated easily as

$$Z = \prod_{i=1}^N \sum_{b_i} e^{\beta \mu b_i} = \left[1 + e^{\beta(\epsilon_b - \epsilon_t)} \right]^N. \quad (16)$$

The mean bond density

$$\langle \phi \rangle = \frac{1}{N} \frac{\partial \ln Z}{\partial (\beta \mu)} = \frac{e^{\beta(\epsilon_b - \epsilon_t)}}{1 + e^{\beta(\epsilon_b - \epsilon_t)}} \quad (17)$$

shows a continuous crossover between a bound (for $\epsilon_b \gg \epsilon_t$) and an unbound (for $\epsilon_b \ll \epsilon_t$) state with $\langle \phi \rangle = 1/2$ for $\epsilon_b = \epsilon_t$.

For a more quantitative analysis of a fluctuating membrane with $\sigma_0 > 0$ we exploit the fact that the effective interactions decay exponentially fast, see Fig. 2. Therefore, we can approximate the bond interactions by taking into account only nearest-neighbors. Moreover, we assume the ligand-receptor pairs to be arranged on a square lattice with spacing a . For an upper bound of the validity of this regime, we choose a lattice spacing $a = \frac{3}{2}\xi$ with $m_1 \equiv m(a) \simeq 0.42$ and interaction energy $\nu = \epsilon_t \chi m_1$. Exploiting the analogy with the lattice gas we can immediately specify the equilibrium phase diagram for independent energies ϵ_b and ϵ_t parametrized by χ , see Fig. 3. Using that at phase coexistence the chemical potential is $\mu_{co} = -4\nu$ and that the critical points obey $\beta\nu^* \simeq 2/2.269$ [28], the line of critical points is determined as

$$\epsilon_b^* = \epsilon_t^* - \frac{\nu^*}{m_1} (1 + 4m_1) \quad (18)$$

with slope one, where the offset depends on m_1 . Specifying χ selects a single critical point. At every critical point, a coexistence line $\epsilon_b(\epsilon_t) = z\epsilon_t$ with slope

$$z \equiv 1 - \chi(1 + 4m_1) \quad (19)$$

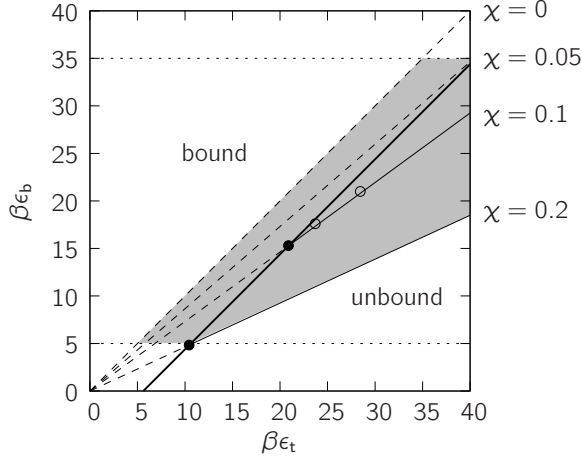


FIG. 3: Set of equilibrium phase diagrams for bonds on a square lattice with nearest-neighbor interactions ($m_1 \simeq 0.42$). Critical points (filled circles) fall on a line (thick line). The shaded region indicates the accessible range of coexistence (solid) and crossover (dashed) lines, and the relevant specific binding energies. In Sec. IV we investigate the dynamics of two state points marked by the open circles for $\chi = 0.1$.

for $\epsilon_t > \epsilon_t^*$ terminates. The straight continuation of the coexistence line below the critical point $\epsilon_t < \epsilon_t^*$ marks the continuous crossover between bound and unbound membrane where $\langle \phi \rangle = 1/2$.

We restrict our discussion to typical values for the specific binding energy ϵ_b ranging from $5k_B T$ to $35k_B T$ [6, 29] as indicated in Fig. 3. The critical point corresponding to the upper limit implies $\chi_1 \simeq 0.05$. Hence, in the range $0 \leq \chi < \chi_1$ for $\epsilon_b \leq 35k_B T$ the qualitative picture for $\chi = 0$ persists and a continuous crossover is observable. For $\chi > \chi_1$ the critical point enters the relevant parameter region and the first order transition becomes accessible. Increasing χ further, the critical point moves down the line given by Eq. (18) to smaller specific binding energies, eventually reaching the lower limit $\epsilon_b^* \simeq 5k_B T$ for $\chi \simeq 0.2$. Hence, the shaded area in Fig. 3 marks the set of coexistence and crossover lines of the effective lattice gas that is compatible with our initial assumption of a small cooperativity parameter χ . A genuine coexistence between closed bonds and open bonds requires both non-negligible membrane fluctuations and rather large specific binding energies ϵ_b and tether energies ϵ_t . For either weak fluctuations or weak binding energies only a continuous crossover between these two states is obtained.

Pushing the analogy with the lattice gas further, in the first order transition regime we estimate the free energy barrier an initially unbound membrane needs to overcome in order to bind to the substrate. From the partition sum (12) we extract the free energy

$$G(\{b_i\}) = \nu \sum_{\langle ij \rangle} (b_i - b_j)^2 - (\epsilon_b - z\epsilon_t) \sum_{i=1}^N b_i,$$

where the sum in the first term runs over all bond pairs. It counts the number of 'broken' links (two neighboring bonds in different states) adding up to the interface length between bound and unbound domains. Assuming a circular domain of size n in the spirit of Becker-Döring [30], the change of free energy associated with this domain is

$$\Delta G(n) \simeq 2\nu\sqrt{\pi n} - (\epsilon_b - z\epsilon_t)n.$$

The critical size of the nucleus and the barrier height are

$$n^\ddagger \simeq \frac{\pi\nu^2}{(\epsilon_b - z\epsilon_t)^2}, \quad \Delta G^\ddagger \simeq \frac{\pi\nu^2}{\epsilon_b - z\epsilon_t},$$

respectively. The nucleation time then grows exponentially with $\beta\Delta G^\ddagger$.

IV. DYNAMICS

Going beyond static properties, in this section we compare the effective bond lattice gas with the full model for the adhesion dynamics close to coexistence. Integrating out the membrane degrees of freedom, one expects the description of bond dynamics through a Markovian stochastic process without memory to be a good approximation in the limit where the formation of bonds is slow compared to the time scale of membrane undulations.

A. Binding and unbinding rates

We start with the implementation of dynamics in the full model. In Fourier space, the membrane modes obey the Langevin equation

$$\partial_t \tilde{h}_{\mathbf{q}} = -\Lambda_{\mathbf{q}} \frac{\partial \mathcal{H}}{\partial \tilde{h}_{\mathbf{q}}^*} + \zeta_{\mathbf{q}}, \quad (20)$$

where $\Lambda_{\mathbf{q}}$ are the Onsager coefficients that take into account the fluid surrounding the membrane [13] and $\zeta_{\mathbf{q}}$ is Gaussian white noise obeying the fluctuation-dissipation theorem. Further details of how the dynamics of the membrane fluctuations is implemented in the full simulation scheme are discussed in Ref. [31, 32].

After a membrane step the heights $h(\mathbf{r}_i)$ are extracted via discrete Fourier transformation and the bonds are updated. The membrane exerts a force f_i on a closed bond that is given by the effective spring constant k times the separation. The unbinding rates for a bond to rupture are then modeled as the usual Bell rates [33],

$$k_i^{\text{off}} = w_0 e^{\beta f_i \sigma_0}, \quad f_i = k[h(\mathbf{r}_i) - l_0] \quad (21)$$

with bare dissociation rate w_0 and effective size of the binding potential set to σ_0 . The binding rates follow through the detailed balance condition as,

$$k_i^{\text{on}} = k_i^{\text{off}} e^{-\frac{1}{2}\beta k[h(\mathbf{r}_i) - l_0]^2 + \beta \epsilon_b}. \quad (22)$$

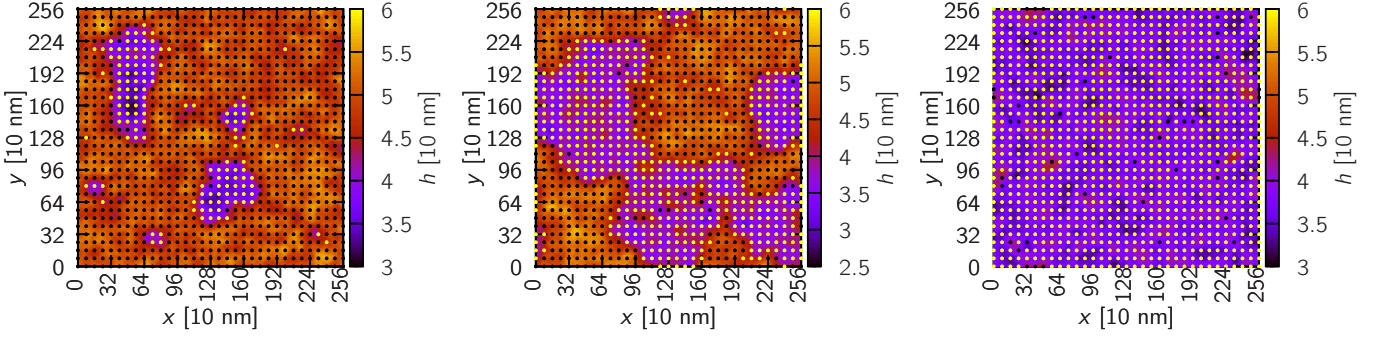


FIG. 4: Membrane height profile and bonds for a single run of an initially unbound membrane: when the critical nucleus has formed (left), when the bond density has reached $\phi \simeq 1/2$ (center), and in equilibrium (right). A closed bond is drawn light, an open bond is dark. Parameters as in Fig. 5b).

These rates are, therefore, independent of the state of other bonds. Cooperative dynamics between bonds, e.g., the assistance of bond formation, are completely due to interactions mediated by the membrane. In Fig. 4, a representative example of the membrane nucleation dynamics of the full model is shown.

For constructing the dynamics in the effective lattice gas, we do not have the explicit height information $h(\mathbf{r}_i)$ of the membrane anymore. The most naive approximation would be to assume a constant unbinding rate. Somewhat more realistically, we can construct an approximation of the membrane force $f_i = k l_i(\{b_i\})$ based on the configuration of neighboring bonds. As a first implementation we will employ a simple linear interpolation $l_i = l(\phi)$ of the bond separation depending only on the bond density ϕ at a given time. The *typical* height of the unbound membrane is h_0 . Force balance between tether force and non-specific interactions for a single closed bond implies

$$a^2 \gamma (h_1 - h_0) + k(h_1 - l_0) = 0$$

for the typical height h_1 of the bound membrane. Linear interpolation then leads to the expression

$$l(\phi) = h_0(1 - \phi) + h_1\phi - l_0 = (h_0 - l_0) \left[1 - \frac{k\phi}{a^2\gamma + k} \right]$$

for the bond separation. Hence, for the unbinding rate we obtain

$$k^{\text{LG,off}}(\phi) = w_0^{\text{LG}} \exp \left\{ \sqrt{\frac{2\beta\nu}{m_1}} \left(1 - \frac{32\chi}{9 + 32\chi} \phi \right) \right\} \quad (23)$$

in the reduced quantities. The rate w_0^{LG} determines the time scale of the lattice gas. Since the membrane undulations slow down the bond formation in the full model, this rate will be smaller than w_0 . The binding rate again follows through detailed balance

$$k_i^{\text{LG,on}} = k^{\text{LG,off}} e^{-\beta\nu \sum_{j(i)} b_j - \beta\mu} \quad (24)$$

and thus depends on the state of the neighboring bonds.

B. Numerics

For the numerical simulations we set the bending rigidity $\beta\kappa = 80$ and the non-specific strength $\beta\gamma = 10^{-5} \text{ nm}^{-4}$. The bond distance is $a = 80 \text{ nm}$ with bond strength $\beta k = 2.25 \times 10^{-2} \text{ nm}^{-2}$. These values lead to height fluctuations $\sigma_0 \simeq 2.1 \text{ nm}$, decay length $\xi \simeq 53.3 \text{ nm}$, and slope $z \simeq 0.73$ of the coexistence line. The cooperativity parameter is $\chi \simeq 0.1$.

In Fig. 5, binding dynamics in the nucleation regime of an initially unbound membrane are compared to the bond lattice gas employing kinetic Monte Carlo moves for two different state points (indicated in Fig. 3). For Fig. 5a) and b), we choose $\beta\epsilon_t \simeq 28.4$ (corresponding to $\beta\nu = 1.2$, $h_0 - l_0 \simeq 50.3 \text{ nm}$) and $\beta\epsilon_b = z\beta\epsilon_t + 0.2 \simeq 21.0$. For Fig. 5c), we move closer towards the critical point with $\beta\epsilon_t \simeq 23.7$ ($\beta\nu = 1$, $h_0 - l_0 \simeq 45.9 \text{ nm}$) and $\beta\epsilon_b = z\beta\epsilon_t + 0.27 \simeq 17.6$. The plotted mean densities $\phi(t)$ are averaged over multiple runs, where single runs are shifted such that at $t = 0$ the critical nucleus has formed. Fig. 5b) shows a system of 256×256 receptor-ligand pairs compared to a 128×128 grid in Fig. 5a). The curves are qualitatively the same for both system sizes, however, the waiting time (not shown) for the critical nucleus to form is much smaller in the bigger system, which is to be expected. The fluctuations of the bound membrane are larger in the full model compared to the lattice gas. For comparison, in Fig. 5b) we show the lattice gas dynamics for constant unbinding rate $k^{\text{LG,off}}(0)$. While it follows the curve of the full model for $\phi < 0.5$, it misses to capture the slowing down of the dynamics for higher bond density. The mean-field rates $k^{\text{LG,off}}(\phi)$ perform much better but still for $\phi > 0.85$ the lattice gas dynamics for the almost bound membrane becomes faster compared to the full model. Moving towards the critical point, dynamics of bond formation slows down as is clearly visible from Fig. 5c).

The bare dissociation rate in the full model is set to $w_0 = 5 \times 10^7 \text{ s}^{-1}$. This rate is close to the inverse relaxation time of membrane undulations on the length scale of the bond distance for the unbound membrane,

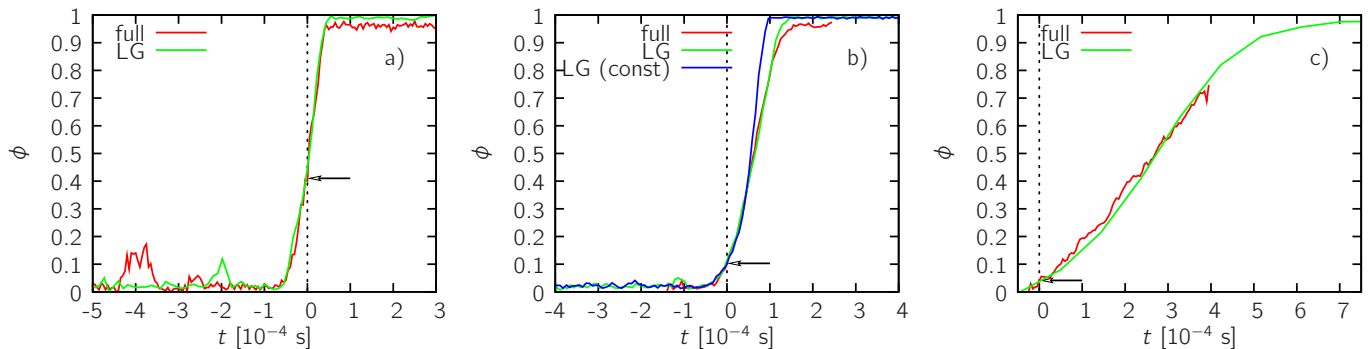


FIG. 5: Dynamics of the lattice gas (LG) compared to the full model for $\chi \simeq 0.1$ (parameters specified in the main text). Shown is the density $\phi(t)$ for an initially unbound membrane in the nucleation regime close to the coexistence line with $\beta\epsilon_t \simeq 28.4$, $\beta\epsilon_b \simeq 21.0$ on a) 128×128 and b) a 256×256 grid. c) Closer to the critical point with $\beta\epsilon_t \simeq 23.7$, $\beta\epsilon_b \simeq 17.6$ on a 256×256 grid. The arrows mark the nucleation barrier $\phi^* = n^*/N$.

$\tau_{\text{un}} \sim \eta a^3 / \kappa \sim 10^{-7} \text{ s}$ with the viscosity of water $\eta \simeq 10^{-3} \text{ Pa} \cdot \text{s}$. Such a correspondence implies that we test a dynamic regime where there is no large time scale separation between membrane undulations and bond formation. Nevertheless, the binding dynamics in Fig. 5 show a very good agreement between full model and lattice gas. Realistic dissociation rates are typically somewhat smaller and, therefore, in a regime where the lattice gas will perform even better. The rates w_0^{LG} have been extracted from scaling the time evolution to fit the full model and have been determined as: $w_0^{\text{LG}}/w_0 \simeq 1.8 \times 10^{-3}$, 2.8×10^{-3} , 2.1×10^{-4} for Fig. 5a)-c), respectively.

V. CONCLUSIONS

Beginning with a Hamiltonian that incorporates the essentials of specific adhesion to a flat substrate, i.e., bending energy of the membrane, a non-specific adhesion potential, and the energy contribution of receptor-ligand pairs, we integrate out the membrane shape in the partition function of the system. In the limit of small membrane roughness and/or weak stiffnesses of the tethers attaching the receptors to the substrate, our approach leads to an effective free energy that is isomorphic to that of a lattice gas model used to describe liquid-gas transitions. We are able to give an explicit expression for the effective interaction potential between bonds. When the bond sites are far enough apart it is sufficient to consider only nearest-neighbor interactions. For bonds on a square lattice the equilibrium phase behavior follows immediately. The analogy to lattice gas models also extends to nucleation theory, yielding expressions for the critical nucleus size of an adhered membrane patch and the energy barrier that needs to be crossed.

We further show that the lattice gas model may also be utilized to study the dynamics of the adhesion process. To this end, we compare simulations of the full Hamiltonian with a kinetic Monte Carlo scheme for the lattice gas. The comparison of results of the computationally

costly simulations of the full model with the fast lattice gas simulations reveals a very good qualitative agreement in the increase of the average bond number as a function of time. We, therefore, expect our model to be useful in more complex studies of, e.g., moving ligands and the influence of defects on membrane adhesion.

TS gratefully acknowledges financial support by the Alexander von Humboldt foundation and the Helios Solar Energy Research Center which is supported by the Director, Office of Science, Office of Basic Energy Sciences of the U.S. Department of Energy under Contract No. DE-AC02-05CH11231. US acknowledges financial support by the DFG under grant SE1119/2. US and ER thank A.-S. Smith for many stimulating discussions and an ongoing fruitful collaboration.

Appendix A: Membrane fluctuations

We expand the height profile $h(\mathbf{r})$ into Fourier modes,

$$h(\mathbf{r}) = \sum_{\mathbf{q}} \tilde{h}_{\mathbf{q}} e^{-i\mathbf{q} \cdot \mathbf{r}}, \quad (\text{A1})$$

where $\tilde{h}_{\mathbf{q}}^* = \tilde{h}_{-\mathbf{q}}$. For a square system of size L , the accessible wave vectors are $\mathbf{q} = (2\pi/L)(n_x, n_y)$ with integer n_x, n_y , and $q \equiv |\mathbf{q}|$. The Helfrich energy (1) becomes

$$\mathcal{H}_0 = \frac{\kappa A}{2} \sum_{\mathbf{q} \neq 0} q^4 |\tilde{h}_{\mathbf{q}}|^2.$$

In the non-specific interactions (2)

$$\mathcal{H}_{\text{ns}} = \frac{\gamma A}{2} \left\{ (\bar{h} - h_0)^2 + \sum_{\mathbf{q} \neq 0} |\tilde{h}_{\mathbf{q}}|^2 \right\}$$

we split off the zero-mode $\bar{h} \equiv \tilde{h}_0$ contribution.

We want to integrate out the fluctuations of the membrane under the constraint that at \mathbf{r}_i the height is

$\bar{h} + \sigma_0 h_i$. This constraint is expressed as

$$\prod_{i=1}^N \delta(h(\mathbf{r}_i) - \sigma_0 h_i) = \frac{1}{(2\pi)^N} \int d\lambda_1 \cdots d\lambda_N \\ \times \exp \left\{ i \sum_{i=1}^N \lambda_i [h(\mathbf{r}_i) - \bar{h} - \sigma_0 h_i] \right\}.$$

In terms of Fourier modes we have

$$h(\mathbf{r}_i) = \bar{h} + \sum'_{\mathbf{q} \neq 0} \left[\tilde{h}_{\mathbf{q}} e^{-i\mathbf{q} \cdot \mathbf{r}_i} + \tilde{h}_{-\mathbf{q}} e^{i\mathbf{q} \cdot \mathbf{r}_i} \right],$$

where the sum $\sum'_{\mathbf{q}}$ runs over independent modes \mathbf{q} (for a \mathbf{q} exclude $-\mathbf{q}$ from the sum). Splitting the coefficient $\tilde{h}_{\mathbf{q}} = \tilde{h}'_{\mathbf{q}} + i\tilde{h}''_{\mathbf{q}}$ into real and imaginary part, the integral over all modes (except the zero-mode) becomes a product of two independent integrals. These are simple Gaussians and read

$$Z' = \prod_{\mathbf{q} \neq 0} d\tilde{h}'_{\mathbf{q}} \\ \times \exp \left\{ - \sum'_{\mathbf{q} \neq 0} \beta A (\kappa q^4 + \gamma) (\tilde{h}'_{\mathbf{q}})^2 + i \sum'_{\mathbf{q} \neq 0} c'_{\mathbf{q}} \tilde{h}'_{\mathbf{q}} \right\}$$

for the integration over real parts. Analogously, Z'' is obtained through replacing $\tilde{h}'_{\mathbf{q}}$ by $\tilde{h}''_{\mathbf{q}}$ and $c'_{\mathbf{q}}$ by $c''_{\mathbf{q}}$. The coefficients are

$$c'_{\mathbf{q}} = 2 \sum_{i=1}^N \lambda_i \cos(\mathbf{q} \cdot \mathbf{r}_i), \quad c''_{\mathbf{q}} = 2 \sum_{i=1}^N \lambda_i \sin(\mathbf{q} \cdot \mathbf{r}_i).$$

The result is

$$Z' Z'' \sim \exp \left\{ - \frac{1}{2} \sigma_0^2 \sum_{ij} m_{ij} \lambda_i \lambda_j \right\}$$

with coupling matrix

$$m_{ij} \equiv \frac{2}{\beta A \sigma_0^2} \sum'_{\mathbf{q} \neq 0} \frac{\cos \mathbf{q} \cdot (\mathbf{r}_i - \mathbf{r}_j)}{\kappa q^4 + \gamma}.$$

We notationally suppress the non-exponential prefactors. The integral over the λ_i implementing the constraints again is a simple multi-dimensional Gaussian integral,

$$\frac{1}{(2\pi)^N} \int d\lambda_1 \cdots d\lambda_N \\ \times \exp \left\{ - \frac{1}{2} \sigma_0^2 \sum_{ij} m_{ij} \lambda_i \lambda_j - i \sum_i \sigma_0 h_i \lambda_i \right\} \\ = [(2\pi)^N \det m]^{-1/2} \exp \left\{ - \frac{1}{2} \sum_{ij} (m^{-1})_{ij} h_i h_j \right\}.$$

The remaining energy is a function of the mean height,

$$E(\bar{h}) \equiv \frac{\gamma A}{2} (\bar{h} - \delta h_0)^2 + \sum_{i=1}^N b_i \left\{ \frac{k}{2} (\bar{h} + \sigma_0 h_i)^2 - \epsilon_b \right\},$$

where we have shifted $\bar{h} \rightarrow \bar{h} + l_0$ for convenience and defined $\delta h_0 \equiv h_0 - l_0$. We finally integrate over the mean height

$$\int d\bar{h} e^{-\beta E(\bar{h})} \simeq e^{-\beta E_b}$$

with

$$E_b = -\frac{1}{2} \frac{(k\sigma_0 \sum_i b_i h_i - \gamma A \delta h_0)^2}{\gamma A + kN\phi} \\ + \frac{\gamma A}{2} (\delta h_0)^2 + \sum_i b_i \left(\frac{k}{2} \sigma_0^2 h_i^2 - \epsilon_b \right). \quad (\text{A2})$$

Appendix B: Effective interaction

To obtain a more useful expression for the bond interactions, we approximate the sum over modes in Eq. (7) by a two-dimensional integral,

$$m(r) = \frac{\xi^4}{2\pi^2 \beta \kappa \sigma_0^2} \int_0^\infty dq \int_0^\pi d\varphi \frac{q \cos[qr \cos \varphi]}{1 + (\xi q)^4} \\ = \frac{\xi^4}{2\pi \beta \kappa \sigma_0^2} \int_0^\infty dq \frac{q J_0(qr)}{1 + (\xi q)^4},$$

where $\xi \equiv (\kappa/\gamma)^{1/4}$ and $J_0(x)$ is the zero-order Bessel function of the first kind. Performing the integral [34] leads to the effective interaction

$$m(r) = -\frac{1}{2\pi \beta \kappa (\sigma_0/\xi)^2} \text{kei}_0(r/\xi) = -\frac{4}{\pi} \text{kei}_0(r/\xi).$$

Since $\text{kei}_0(0) = -\pi/4$ we have $m(0) = 1$. Here, $\text{kei}_0(x)$ is a Kelvin function defined as

$$\text{kei}_0(x) \equiv \text{Im} K_0(x e^{i3\pi/4}), \quad (\text{B1})$$

where $K_0(z)$ is the zero-order modified Bessel function of the second kind.

-
- [1] M. C. Beckerle, ed., *Cell Adhesion* (Oxford University Press, Oxford, 2001), 1st ed.
 - [2] D. A. Lauffenburger and J. Linderman, *Receptors: Models for Binding, Trafficking, and Signaling* (Oxford University Press, 1995).
 - [3] D. A. Hammer and M. Tirrell, *Annu. Rev. Mater. Sci.* **26**, 651 (1996).
 - [4] P. Bongrand, *Rep. Prog. Phys.* **62**, 921 (1999).
 - [5] J. Y. Wong and T. L. Kuhl, *Langmuir* **24** (2008).
 - [6] D. H. Boal, *Mechanics of the Cell* (Cambridge University Press, 2002), 1st ed.
 - [7] M. Tanaka and E. Sackmann, *Nature* **437**, 656 (2005).
 - [8] D. Cuvelier and P. Nassoy, *Phys. Rev. Lett.* **93**, 228101 (2004).
 - [9] K. Mossman and J. Groves, *Chem. Soc. Rev.* **36**, 46 (2007).
 - [10] A.-S. Smith and E. Sackmann, *ChemPhysChem* **10**, 66 (2009).
 - [11] K. Sengupta and L. Limozin, *Phys. Rev. Lett.* **104**, 088101 (2010).
 - [12] W. Helfrich, *Z. Naturforsch.* **33a**, 305 (1978).
 - [13] U. Seifert, *Adv. Phys.* **46**, 13 (1997).
 - [14] R. Lipowsky, *Handbook of Biological Physics* **1**, 521 (1995).
 - [15] R. Lipowsky, *J. Phys. II France* **4**, 1755 (1994).
 - [16] R. Lipowsky and S. Leibler, *Phys. Rev. Lett.* **56**, 2541 (1986).
 - [17] E. Sackmann and R. F. Bruinsma, *ChemPhysChem* **3**, 262 (2002).
 - [18] S. Komura and D. Andelman, *Europhys. Lett.* **64**, 844 (2003).
 - [19] R. Lipowsky, *Phys. Rev. Lett.* **77**, 1652 (1996).
 - [20] T. Weikl, D. Andelman, S. Komura, and R. Lipowsky, *Eur. Phys. J. E* **8**, 59 (2002).
 - [21] D. M. Zuckerman and R. F. Bruinsma, *Phys. Rev. E* **57**, 964 (1998).
 - [22] T. R. Weikl, R. R. Netz, and R. Lipowsky, *Phys. Rev. E* **62**, R45 (2000).
 - [23] C.-Z. Zhang and Z.-G. Wang, *Phys. Rev. E* **77**, 021906 (2008).
 - [24] T. R. Weikl and R. Lipowsky, *Phys. Rev. E* **64**, 011903 (2001).
 - [25] T. R. Weikl, M. Asfaw, H. Krobath, B. Rozycki, and R. Lipowsky, *Soft Matter* **5**, 3213 (2009).
 - [26] F. L. Brown, *Ann. Rev. Phys. Chem.* **59**, 685 (2008).
 - [27] E. Reister-Gottfried, K. Sengupta, B. Lorz, E. Sackmann, U. Seifert, and A.-S. Smith, *Phys. Rev. Lett.* **101**, 208103 (2008).
 - [28] D. Chandler, *Introduction to Modern Statistical Mechanics* (Oxford University Press, Oxford, 1987).
 - [29] G. Weber, *Adv. Prot. Chem.* **29**, 1 (1975).
 - [30] R. Becker and W. Döring, *Ann. Phys.* **24**, 719 (1935).
 - [31] E. Reister-Gottfried, S. M. Leitenberger, and U. Seifert, *Phys. Rev. E* **75**, 011908 (2007).
 - [32] E. Reister, U. Seifert, and A. Smith, p. in preparation (2010).
 - [33] G. I. Bell, *Science* **200**, 618 (1978).
 - [34] Gradshteyn and Ryzhik, *Table of Integrals, Series, and Products* (Academic Press, 2007), seventh ed.